Synthesis, Conformational Isomerism, and Fluxional Behavior of Octahedral Bis(alkyne)tungsten(0) Complexes

Tsung-Yu Hsiao, Pei-Lung Kuo, Chen-Hsing Lai, Chien-Hong Cheng,* Chih-Yi Cheng, and Sue-Lein Wang*

Department of Chemistry, National Tsing Hua University, Hsinchu, Taiwan 300, Republic of China

Received November 12, 1992

trans-Bis(alkyne)tungsten complexes $W(CO)_2(NN)(RC{\equiv}CR')_2$ (1–4) were synthesized via the exchange reaction of $W(CH_3CN)_3(CO)_3$ with 1 equiv of chelate nitrogen ligand NN and 2 equiv of alkyne, where NN = bpy (**a**), phen (**b**), 4-Mephen (**b'**), en (**c**), 2-(NH_2CH_2)py (**d**) and RC≡CR' = MeO_2CCCCO_2Me (**1**), $PhCCCO_2Et$ (**2**), $HCCCO_2Me$ (**3**), $HCCCO_2Et$ (**4**), at ambient temperature. The solid-state structure of a representative of the series, **2a** (NN = bpy, RC≡CR' = $PhCCCO_2Et$) was determined by the X-ray diffraction method. The results indicate that the geometry of the compound is octahedral, with the two CO groups cis to each other but each trans to a pyridyl group, while the two $PhCCCO_2Et$ ligands are trans to each other and are cis to the CO and the bpy ligands. The two alkynes are mutually orthogonal, and each eclipses a N–M–C vector. In addition, the X-ray study shows that the phenyl end of the alkyne ligand is close to the CO group and the ester group is near the bpy ligand. This compound crystallizes in the monoclinic space group *Cc* with unit cell dimensions a = 15.523(5) Å, b = 9.676(2) Å, c = 21.471(6) Å, and β = 108.17(2)° for Z = 4. According to variable-temperature NMR spectra, complexes **2–4** exist in solution as a mixture of conformational isomers arising from different orientations of the unsymmetric alkyne ligands relative to the N–W–CO vectors. For **2a** and **2b**, the three conformational isomers **A–C** were detected at low temperatures, although only conformation **A** was observed in the solid state. For complexes **3a,b** and **4a,b**, only conformations **A** and **B** were found, but for the en complex **2c**, only **A** was observed in the low-temperature NMR spectra of these complexes. Several mechanisms have been considered for the observed dynamic NMR behavior of these complexes. A dissociative process involving the exchange of free and coordinated alkynes has been eliminated. Nondissociative mechanisms involving a concerted disrotatory motion and an independent motion of the alkyne ligands also cannot account for all observations. Only the mechanism of conrotatory motion of the two alkyne ligands is in agreement with all experimental facts.

Introduction

Octahedral molybdenum and tungsten complexes containing two trans π-ligands, including alkenes,[1] alkynes,[2] dioxygens,[3] and carbon dioxide,[4] have attracted considerable attention both theoretically and experimentally. The main focus has generally been on the conformation and mechanism of rotation of the two trans π-ligands. Molecular orbital analysis of $ML_4(\pi\text{-ligand})_2$ has indicated that electronically the two trans π-ligands strongly favor being mutually orthogonal, but each π-ligand tends to eclipse a L–M–L vector. With respect to the mechanism of rotation of the two trans π-ligands, Veillard et al. have shown, in the model complex *trans*-$Mo(PH_3)_4(C_2H_4)_2$, the process in which each ethylene ligand rotates independently is more favorable than that with both ethylenes rotating synchronously in the same direction, but in *trans*-$Mo(CO)_4(C_2H_4)_2$, the activation energy of the latter process is slightly smaller than that of the former.[5] On the other hand, according to both theoretical[6] and experimental[7] investigations on the mechanism of CO_2 rotation in *trans*-bis(carbon dioxide)molybdenum complexes conrotatory motion of CO_2 ligands operates.

Our interests in transition-metal-catalyzed alkyne chemistry[8] led us to synthesize the first trans molybdenum bis(alkyne) complexes, $Mo(CO)_2(NN)(DMAC)_2$ (NN = bpy, phen; DMAC = MeO_2CCCCO_2Me).[2a] These and $W(CO)_2$(dppe)$(DMAC)_2$[2b] are the only three octahedral d^6 bis(alkyne) complexes that have been reported to date. As predicted theoretically, the trans alkynes in these complexes are staggered to each other, but each alkyne eclipses one P–W–CO vector in $W(CO)_2$(dppe)$(DMAC)_2$ or one N–Mo–CO vector in $Mo(CO)_2(NN)(DMAC)_2$. In addition, the variable-temperature NMR spectra of these complexes show fluxional behavior due to the rotation of the DMAC ligands. The mechanism of the alkyne rotation, however, is not yet understood. It is interesting to note that a

(1) (a) Byrne, J. W.; Blaser, H. V.; Osborn, J. A. *J. Am. Chem. Soc.* **1975**, *97*, 3871. (b) Carmona, E.; Marin, J. M.; Poveda, M. L.; Atwood, J. L.; Rogers, R. D. *J. Am. Chem. Soc.* **1983**, *105*, 3014. (c) Stolz, I. W.; Dobson, G. R.; Sheline, R. K. *Inorg. Chem.* **1963**, *2*, 1264.

(2) (a) Lain, L. S.; Cheng, C. H.; Cheng, C. Y.; Wang, S. L. *J. Organomet. Chem.* **1990**, *390*, 330. (b) Birdwhitstell, K. R.; Tonker, J. L.; Templeton, J. L. *J. Am. Chem. Soc.* **1987**, *109*, 1401.

(3) Chevrier, B.; Diebold, Th.; Weiss, R. *Inorg. Chim. Acta* **1976**, *19*, L57.

(4) (a) Alvarez, R.; Carmona, E.; Poveda, M. L.; Sánchez-Delgado, R. *J. Am. Chem. Soc.* **1984**, *106*, 2731. (b) Alvarez, R.; Carmona, E.; Marin, J. M.; Poveda, M. L.; Gutiérrez-Puebla, E.; Monge, A. *J. Am. Chem. Soc.* **1986**, *108*, 2286. (c) Carmona, E.; Muñoz, M. A.; Pérez, P. J.; Poveda, M. L. *Organometallics* **1990**, *9*, 1337.

(5) Bachmann, C.; Demuynck, J.; Veillerd, A. *J. Am. Chem. Soc.* **1978**, *100*, 2366.

(6) Sánchez-Marcos, E.; Caballol, R.; Trinquieer, G.; Bartherlat, J. C. *J. Chem. Soc., Dalton Trans.* **1987**, 2373.

(7) Carmona, E.; Hughes, A. K.; Munoz, M. A.; O'Hare, D. M.; Perez, F. J.; Poveda, M. L. *J. Am. Chem. Soc.* **1991**, *113*, 9210.

(8) (a) Kong, K. C.; Cheng, H. C. *J. Chem. Soc., Chem. Commun.* **1991**, 423. (b) Duan, I. F.; Cheng, H. C. *J. Chem. Soc., Chem. Commun.* **1991**, 1347. (c) Kong, K. C.; Cheng, H. C. *Organometallics* **1992**, *11*, 1972.

0276-7333/93/2312-1094$04.00/0

Table I. Characterization Data for *trans*-W(NN)(CO)$_2$(RCCR')$_2$

complex	IR, cm^{-1} ν(CO)	IR, cm^{-1} ν(CC)	^{13}C NMR, ppm[a] C≡C
W(bpy)(CO)$_2$(DMAC)$_2$ (**1a**)	2010, 1940	1775	137.49, 149.20
W(phen)(CO)$_2$(DMAC)$_2$ (**1b**)	2013, 1945	1769	141.36, 150.48
W(en)(CO)$_2$(DMAC)$_2$ (**1c**)	2011, 1937	1741	148.21, 151.34
W(2-NH$_2$CH$_2$py)(CO)$_2$(DMAC)$_2$ (**1d**)	2011, 1938	1746	
W(bpy)(CO)$_2$(PhCCCO$_2$Et)$_2$ (**2a**)	1988, 1915	1739	139.27, 147.44
W(phen)(CO)$_2$(PhCCCO$_2$Et)$_2$ (**2b**)	1984, 1909	1736	139.21, 148.07
W(4-Mephen)(CO)$_2$(PhCCCO$_2$Et)$_2$ (**2b'**)	1982, 1908	1736	
W(en)(CO)$_2$(PhCCCO$_2$Et)$_2$ (**2c**)	1981, 1907	1725	137.63, 139.79
W(2-NH$_2$CH$_2$py)(CO)$_2$(PhCCCO$_2$Et)$_2$ (**2d**)	1982, 1908	1727	
W(bpy)(CO)$_2$(HCCCO$_2$Me)$_2$ (**3a**)	1978, 1901	1724	136.32, 141.40
W(phen)(CO)$_2$(HCCCO$_2$Me)$_2$ (**3b**)	1973, 1896	1723	134.95, 143.76
W(4-Mephen)(CO)$_2$(HCCCO$_2$Me)$_2$ (**3b'**)	1974, 1898	1718	
W(bpy)(CO)$_2$(HCCCO$_2$Et)$_2$ (**4a**)	1976, 1899	1721	134.07, 141.40
W(phen)(CO)$_2$(HCCCO$_2$Et)$_2$ (**4b**)	1977, 1900	1719	134.27, 142.67

[a] Spectra were recorded in CD_2Cl_2 at 243 K.

number of bis(alkyne) compounds have been reported, but nearly all of the known bis(alkyne) compounds are in the d^4 configuration with the two alkyne ligands cis and approximately parallel to each other. Examples of early-transition-metal bis(alkyne) complexes include (π-C$_5$H$_5$)M(CO)(PhC≡CPh)$_2$ (M = V, Nb, Ta),[9] (π-C$_5$H$_5$)M(RC≡CR)$_2$X (M = Mo, W),[10] Mo(R^{1}C≡CR^2)$_2$(S$_2$CNR$_2$)$_2$,[11] [W(CO)(NCMe)(S$_2$CNC$_4$H$_8$)(MeC≡CMe)$_2$](BPh$_4$),[12] and WI(CO)(R^{1}C≡CR^2)$_2$(S$_2$CNR$_2$).[13] The cis and parallel structure allows the two alkyne filled $\pi_\perp$ orbitals (perpendicular to the MC$_2$ plane) to interact with the same vacant metal d$_\pi$ orbital and thus stabilize the complex.[14]

Octahedral d^6 bis(alkyne) complexes are expected to be less stable in view of the presence of the repulsion between filled d$_\pi$ and $\pi_\perp$ orbitals. In order to explore the scope of this chemistry, to understand the fluxional behavior of the *trans*-bis(alkyne) complexes, and to compare the mechanism with those for ethylene and carbon dioxide rotation, we undertook the present studies. In this paper, unsymmetric alkynes were successfully employed for the synthesis of several new *trans*-bis(alkyne)tungsten complexes. The directional selectivity of these ligands led to the observation of a thermodynamic mixture of conformational isomers in solution in the variable-temperature NMR spectra. Most importantly, the NMR results allow us to elucidate clearly the mechanism of the alkyne rotation.

Results

Synthesis of *trans*-W(CO)$_2$(NN)(RCCR')$_2$. The *trans*-bis(alkyne) complexes were prepared from W(CO)$_3$(CH$_3$CN)$_3$ in two steps. Treatment of the tungsten acetonitrile complex with 1 equiv of the bidentate ligand NN (2,2'-bipyridine and 1,10-phenanthroline) at ambient temperature generated in situ a new tungsten species, W(CO)$_3$(NN)(CH$_3$CN). Subsequent addition of 2 equiv of the alkyne ligand led to the formation of the desired product. A series of tungsten bis(alkyne) complexes were prepared by this method, as summarized in eq 1 (bpy = 2,2'-bipyridine, phen = 1,10-phenanthroline, en = ethylenediamine, py = pyridine).

$$\mathrm{W(CO)_3(CH_3CN)_3} \xrightarrow{\mathrm{NN}} \mathrm{W(CO)_3(NN)(CH_3CN)} \xrightarrow{\mathrm{RC{\equiv}CR'}} \textit{trans}\text{-}\mathrm{W(CO)_2(NN)(RC{\equiv}CR')_2} \quad (1)$$

1–4

R = CO_2Me, R' = CO_2Me, NN = bpy (**1a**), phen (**1b**), en (**1c**), 2-NH$_2$CH$_2$py (**1d**)

R = Ph, R' = CO_2Et, NN = bpy (**2a**) phen (**2b**), 4-Mephen (**2b'**), en (**2c**), 2-NH$_2$CH$_2$py (**2d**)

R = H, R' = CO_2Me, NN = bpy (**3a**), phen (**3b**), 4-Mephen (**3b'**)

R = H, R' = CO_2Et, NN = bpy (**4a**), phen (**4b**)

A modified method was employed for the synthesis of *trans*-W(CO)$_2$(NN)(PhCCCO$_2$Et)$_2$ (**2d**), where NN = 2-NH$_2$CH$_2$py (2-(aminomethyl)pyridine). The reaction of W(CO)$_3$(CH$_3$CN)$_3$ with 2 equiv of 4-Mepy (4-methylpyridine) in CH$_3$CN led to the generation in situ of W(CO)$_3$(4-Mepy)$_2$(CH$_3$CN). Addition of 2 equiv of PhCCCO$_2$Et resulted in the precipitation of the brown solid W(CO)$_2$(4-Mepy)$_2$(PhCCCO$_2$Et)$_2$. The complex was thermally stable in the solid state, but it decomposed rapidly in solution at ambient temperature. Complex **2d** was then obtained by substitution of the two pyridine ligands in W(CO)$_2$(4-Mepy)$_2$(PhCCCO$_2$Et)$_2$ with 2-NH$_2$CH$_2$py at ambient temperature. In all the reactions of W(CO)$_3$(NN)(CH$_3$CN) and W(CO)$_3$(4-Mepy)$_2$(CH$_3$CN) with the alkynes listed in eq 1, the mono(alkyne) complexes W(CO)$_3$(NN)(alkyne) and W(CO)$_3$(4-Mepy)$_2$(alkyne) were not detected. The new complexes **1–4** were characterized by IR and NMR spectroscopy and microanalysis. As shown in Table I, all these species exhibit in the IR spectra two strong absorptions at 1973–2013 and 1896–1945 cm^{-1} characteristic of cis dicarbonyls and a broad absorption

(9) Nesmeyanov, A. I.; Gusev, A. I.; Pasynskii, A. A.; Amisimov, K. N.; Kolobova, N. E.; Struchkov, Yu. T. *J. Chem. Soc. D* **1969**, 277.

(10) (a) Faller, J. W.; Murray, H. H. *J. Organomet. Chem.* **1979**, *172*, 171. (b) Davidson, J. L.; Green, M.; Stone, F. G. A.; Welch, A. J. *J. Chem. Soc., Dalton Trans.* **1976**, 738. (c) Watson, P. L.; Bergman, R. G. *J. Am. Chem. Soc.* **1980**, *102*, 2698. (d) O'Regan, M. B.; Vale, M. G.; Payack, V. J.; Shrock, R. R. *Inorg. Chem.* **1992**, *31*, 1112. (e) Thomas, J. L. *Inorg. Chem.* **1978**, *17*, 1507.

(11) (a) Herrick, R. S.; Templeton, J. L. *Organometallics* **1982**, *1*, 842. (b) McDonald, J. W.; Newton, W. E.; Creedy, C. T. C.; Corbin, J. L. *J. Organomet. Chem.* **1975**, *92*, C25.

(12) Baker, P. K.; Drew, M. G. B.; Flower, K. R. *J. Organomet. Chem.* **1990**, *391*, C12.

(13) (a) Armstrong, E. M.; Baker, P. K.; Flower, K. R.; Drew, M. G. B. *J. Chem. Soc., Dalton Trans.* **1990**, 1535. (b) Davidson, J. L.; Vasapollo, G. *J. Chem. Soc., Dalton Trans.* **1988**, 2855.

(14) Herrick, R. S.; Templeton, J. L. *Organometallics* **1982**, *1*, 842.

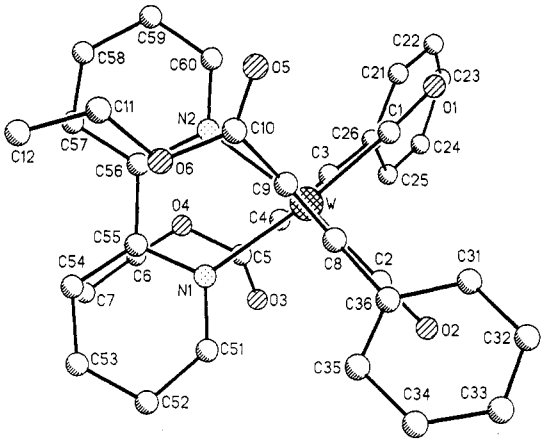

Figure 1. ORTEP drawing of $W(bpy)(CO)_2(PhCCCO_2Et)_2$ (**2a**) showing the scheme of atom labeling.

at 1718–1769 cm^{-1} and in the ^{13}C NMR spectra two resonances at 134–152 ppm for the carbon–carbon triple bonds.

X-ray Structure of $W(CO)_2(bpy)(PhCCCO_2Et)_2$ (2a). The structures of complexes **1–4** are expected to be similar to those of $W(CO)_2(dppe)(DMAC)_2$ and $Mo(CO)_2(bpy)(DMAC)_2$ (DMAC = dimethyl acetylenedicarboxylate) with the two alkyne ligands being staggered with respect to each other and each alkyne ligand eclipsing an N–M–C vector. However, due to the unsymmetrical nature of the alkyne ligands in complexes **2–4**, each of these alkynes may have two possible arrangements as it lies on an N–M–C vector, one with the ester group near the nitrogen atom and the other with the ester close to the carbon atom. It appears impossible to assign confidently the conformation of these alkyne ligands from the spectral data of the complexes. Thus, a representative of these series, **2a**, was selected for structural determination by X-ray diffraction methods. An ORTEP diagram of the complex with atomic numbering is presented in Figure 1, while important intramolecular bond distances and bond angles are shown in Table II. The geometry of compound **2a** is octahedral, with the two CO groups cis to each other but each trans to a pyridyl group, while the two PhCCCOOEt ligands are trans to each other and are cis to the CO and the bpy ligands. These structural results confirm that the two alkynes are mutually orthogonal (88.2°) and each alkyne ligand eclipses an N–M–C vector (6.7°). In addition, the results also show that the phenyl end of each alkyne ligand is close to the CO group and the ester group is near the bpy ligand.

Dynamic NMR Behavior of *trans*-$W(CO)_2(NN)(DMAC)_2$ (1a–c). NMR spectra of compound **1a** at various temperatures indicate it is a fluxional molecule. ^1H NMR spectra at low temperatures are consistent with a static structure similar to $Mo(CO)_2(bpy)(DMAC)_2$, as evidenced by the observation of two methyl resonances at δ 3.15 and 3.76 at 243 K. The former is assigned to the methyl groups near the bpy ligand, whereas the latter is due to the methyl protons close to the carbonyl groups (vide infra). As the temperature was raised above 263 K, rotation of the DMAC ligands took place and broadening of the two methyl signals was observed. At 300 K, the two resonances coalesce and a broad signal at δ 3.47 was observed for the methyl protons. When the temperature was raised, the signal became sharper and the fast-exchange limit was reached at temperatures above 343 K. Variable-temperature ^{13}C NMR studies of compound **1a**

Table II. Important Bond Lengths (Å) and Angles (deg) for of 2a

W–N(1)	2.244(18)	W–N(2)	2.226(15)
W–C(1)	1.965(20)	W–C(2)	1.948(27)
W–C(3)	2.130(19)	W–C(4)	2.184(27)
W–C(8)	2.211(20)	W–C(9)	2.108(34)
O(1)–C(1)	1.149(26)	O(2)–C(2)	1.189(31)
O(3)–C(5)	1.182(34)	O(4)–C(5)	1.341(24)
O(5)–C(10)	1.139(32)	O(6)–C(10)	1.305(24)
C(3)–C(4)	1.287(31)	C(3)–C(26)	1.479(27)
C(4)–C(5)	1.396(35)	C(8)–C(9)	1.237(36)
C(8)–C(36)	1.497(27)	C(9)–C(10)	1.508(41)
N(1)–W–N(2)	72.2(6)	N(1)–W–C(1)	165.5(8)
N(2)–W–C(1)	103.2(7)	N(1)–W–C(2)	99.5(9)
N(2)–W–C(2)	167.7(10)	C(1)–W–C(2)	87.0(10)
N(1)–W–C(3)	115.9(7)	N(2)–W–C(3)	87.9(7)
C(3)–W–C(4)	34.7(8)	N(1)–W–C(8)	84.1(7)
C(2)–W–C(8)	75.0(10)	C(3)–W–C(8)	155.8(8)
C(4)–W–C(8)	156.2(9)	N(1)–W–C(9)	80.1(10)
N(2)–W–C(9)	80.0(9)	C(1)–W–C(9)	85.6(11)
C(2)–W–C(9)	108.1(11)	C(3)–W–C(9)	156.0(10)
C(4)–W–C(9)	156.8(10)	C(8)–W–C(9)	33.2(10)
W–N(1)–C(55)	120.5(12)	W–N(2)–C(56)	117.2(11)
W–C(1)–O(1)	175.7(17)	W–C(2)–O(2)	174.9(24)
W–C(3)–C(4)	74.9(14)	W–C(3)–C(26)	149.6(16)
C(4)–C(3)–C(26)	134.9(22)	W–C(4)–C(3)	70.4(15)
W–C(4)–C(5)	145.5(16)	C(3)–C(4)–C(5)	144.0(23)
W–C(8)–C(9)	68.8(17)	W–C(8)–C(36)	142.1(17)
C(9)–C(8)–C(36)	149.0(26)	W–C(9)–C(8)	78.0(20)
W–C(9)–C(10)	141.5(18)	C(8)–C(9)–C(10)	140.5(27)

revealed further information about its dynamic behavior. Below 243 K, the complex may be considered as static and carbon nuclei of each type on the DMAC appeared as pairs (δ 179.0 and 179.1 for COO; δ 137.5 and 149.2 for C≡; δ 52.3 and 51.1 for CH_3) in the spectrum. For other carbon nuclei in the complex, only one resonance was observed for each type in accordance with the proposed structure. At higher temperature, rotation of DMAC ligands became rapid and broadening of the carbon signals on the DMAC ligands occurred. Due to the result of broadening, the resonances corresponding to the acetylene carbon were difficult to observe in the temperature range 273–343 K. As the temperature was raised up to higher than 353 K, the fast-exchange regime was reached and only one resonance was observed for carbon nuclei of each type on the DMAC ligands. For the other ^{13}C NMR signals, there appeared no significant change throughout the entire temperature range. A similar dynamic behavior was observed for compounds **1b,c**. From the results of variable-temperature NMR spectra, the barriers of alkyne rotation for **1a–c** were calculated to be 13.2, 13.3, and 14.2 kcal/mol, respectively. The ^1H and ^{13}C chemical shifts of **1a–c** at ambient temperature are presented in the Experimental Section.

Dynamic NMR Behavior of *trans*-$W(CO)_2(NN)(PhCCCO_2Et)_2$ (2a–c). Variable-temperature NMR studies of compounds **2a,b** have demonstrated rather complex dynamic behavior of these molecules in solution. Theoretically, the three conformational isomers **A–C** may exist for these complexes if the conformations of the two trans alkynes remain orthogonal and eclipsed. Indeed, the ^1H NMR spectra of complex **2b** at various temperatures in CD_2Cl_2 as shown in Figure 2 can be explained on the basis of the existence of a thermodynamic mixture of the three rotational isomers **2b-A–C**. At 193 K, the complex is static and each resonance observed at 298 K is split into four signals due to the presence of the three rotational isomers. For instance, the resonance at δ 9.22 (d) for H-2,9 of the phen ligand at room temperature now appears at

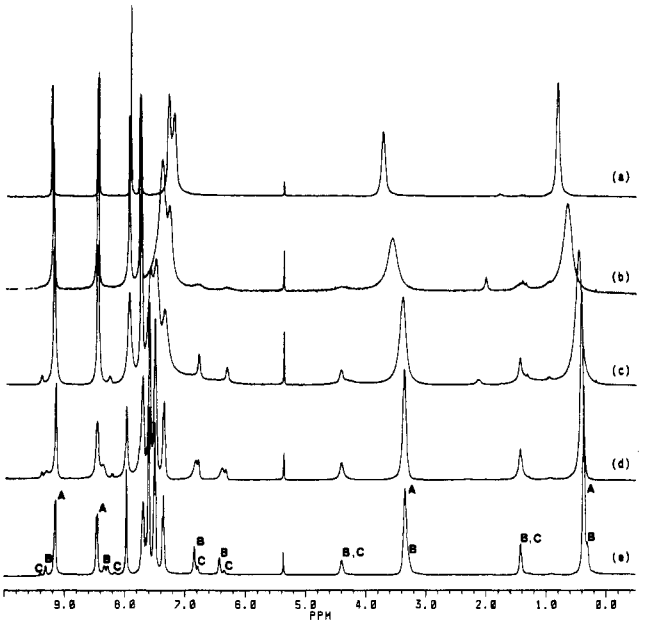

Figure 2. ^{1}H NMR spectra of W(phen)(CO)$_2$(PhCCCO$_2$Et)$_2$ (**2b**) in CD_2Cl_2 at various temperatures: (a) 293 K; (b) 253 K; (c) 233 K; (d) 213 K; (e) 193 K.

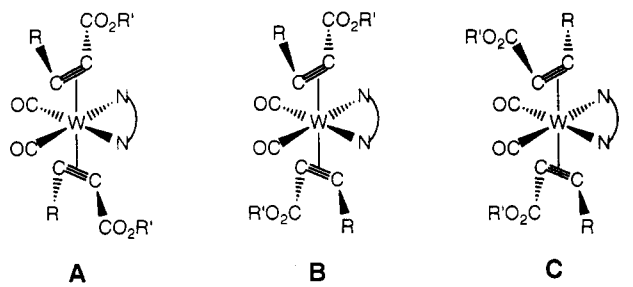

δ 9.38, 9.30, 9.15, and 9.14 with relative intensities 1:2.7:2.7:19. As **2b** adopts structure **A** in the solid state, we assign this structure to the major isomer (δ 9.14). The signals at δ 9.30 and 9.15 (overlapping partially with the major signal at δ 9.14) correspond to isomer **2b-B**, in which one ester group on the alkyne ligands is near a carbonyl group and the other is close to the phen ligand. In this isomer, the two ortho protons H-2 and H-9 of the phen ligand no longer have the same environment due to the difference in direction of the two alkynes relative to the N–W–C vectors. Consequently, they appear as two separate resonances of equal intensity. Finally, the weak resonance at δ 9.38 is assigned to the minor isomer **C** with both phenyl groups of the alkyne ligands near the coordinated phen and both ester groups lying over the carbonyl ligands. The H-4 and H-7 signal of the phen ligand at δ 8.45 (d) at ambient temperature is also split into four resonances at δ 8.45, 8.32, 8.26, and 8.14 with relative intensities 19:2.7:2.7:1 at 193 K. These resonances correspond to the three structures **2b-A** (δ 8.45), **2b-B** (δ 8.32, 8.26), and **2b-C** (δ 8.14). Other signals of **2b** also split similarly, although in some cases the signals overlap with each other due to a small difference of chemical shift. From the peak intensities, the relative populations of **2b-A–C** were calculated to be 19:5.5:1 at 193 K. Similar dynamic NMR behavior was also observed for **2a**. There was only one set of signals in the ^{1}H NMR spectrum at 298 K, but as the temperature was lowered to 193 K, the slow-exchange limit regime was reached and the NMR spectrum revealed the presence of three conformational isomers **2a-A–C** with relative intensities 12:4:1. In sharp contrast to the fluxional behavior of **2a** and **2b**, investigation of complex **2c** by NMR in the temperature range 193–373 K has demonstrated simple behavior. There is only one set of signals corresponding to conformer **2c-A** observed throughout the entire temperature range. The concentration of conformers **B** and **C** for complex **2c** appeared too low to be seen.

Effects of Ring Current. In the ^{1}H NMR spectra of complexes **2a** and **2b** at low temperatures, unusual upfield shifts for the ethyl resonances of conformer **A** and one ethyl resonance of conformer **B** were observed. For **2b** as the example (Figure 2), the resonances of the two ethyl groups in **2b-A** appear at δ 0.37 (CH_3) and 3.34 (CH_2), and one ethyl group in **2b-B** produces signals at δ 0.31 (CH_3) and 3.28 (CH_2), whereas the other ethyl group in **2b-B** and the two ethyl groups in **C** appear at δ 1.42 and 4.39 for CH_3 and CH_2, respectively. Differences of chemical shift exceeding 1 ppm were observed for both the methyl and methylene resonances. All those ethyl protons in the upper field regions are assigned to PhCCCO$_2$Et ligands with the ester groups close to the coordinated phen, in view of the fact that these ester groups, being located right above or below the phen ring, are thus markedly affected by the ring current. In conformers **B** and **C** of **2b**, at least one phenyl group of the acetylene ligands lies on the coordinated phen. A similar ring current effect of the phen ligand also to significant upfield shift of these phenyl resonances. The proton resonances of the phenyl groups of **2b-A** that are unaffected by the ring current of phen appear at δ 7.59 (d), 7.49 (t), and 7.34 (t) for the ortho, meta, and para protons, while the signals due to the phenyl protons of **2b-B** lying above the phen ligand shift to δ 6.84 (3 H) and 6.44 (2 H) and the phenyl protons of **2b-C** to 6.78 (3 H) and 6.35 (2 H). Unambiguous assignments of these resonances cannot confidently be made because of the lack of coupling information (Figure 2). The effect of ring current on the chemical shift of the PhCCCO$_2$Et ligands of complex **2a** was also observed, although the difference in chemical shift caused by the ring current imparted by bpy was smaller in this complex. For complex **2c**, in which no aromatic ring in the NN ligand is present, the NMR resonances of the ethyl protons on the coordinated PhCCCO$_2$Et are at δ 1.39 and 4.31. These values are also more than 1 ppm downfield relative to the corresponding chemical shifts of **2b-A**. Analysis of the ^{1}H NMR data of the DMAC complexes **1a–c**, also reveals significant ring current effect on the chemical shift of the methyl groups. At ambient temperature, only one methyl resonance is observed for each species because of the rapid rotation of DMAC ligands (vide supra); these resonances appear at δ 3.52, 3.42, and 3.80 for **1a–c**, respectively. Once again, the ring-current effect decreases in the order phen > bipy > en.

Dynamic NMR Behavior of W(CO)$_2$(NN)(HCCCO$_2$R)$_2$ (3a,b,b′ and 4a,b). One interesting NMR property of complexes **3** and **4** is the observation of extremely downfield signals at ca. δ 9.4 for the acetylenic protons in the ^{1}H NMR spectra of these complexes. For reference, the chemical shift of the acetylenic proton in the free HCCCO$_2$R (R = Me, Et) appears at δ 2.9. A downfield shift of 6.5 ppm occurs as the propiolate ligands are bonded to the W(0) center.

^{1}H NMR spectra of species **3** and **4**, unlike those of complexes **2a,b**, show conformational isomers of only two types, **A** and **B**, at low temperature. The concentration

of conformer **C** is too low to be seen. Presumably, the arrangement of the propiolate ligands with both ester groups close to the CO group and the hydrogen close to the nitrogen ligand is strongly disfavored. For complex $W(CO)_2(phen)(HCCCO_2Et)_2$ (**4b**), structure **4b-A**, in which the electron-withdrawing ester groups are close to the nitrogen ligands, is assigned as the major conformer. The assignment is based on the X-ray results for complex **2a** and a comparison of ^1H NMR spectra with those of **2a**. A key piece of evidence from the spectra supporting the assignment is that the chemical shifts of the ethyl protons of this major isomer at the slow-exchange limit are all ca. 1 ppm upfield relative to the corresponding signals of the free ligand, indicating that the ethyl protons are under the influence of the ring current from the phen ligand. The minor conformational isomer **4b-B** was identified by the presence of two resonances at δ 9.51 (s) and 8.42 (s) for the acetylenic protons and δ 9.11 (d) and 9.03 (d) for protons ortho to the nitrogen atoms of the phen ligand. On the basis of the known ring-current effect of the phen ligand, the acetylenic resonance at δ 8.42 was attributed to the first $HCCCO_2Et$ ligand with its acetylenic proton close to the phen ligand, whereas the resonance at δ 9.51 was assigned to the second $HCCCO_2Et$, the acetylenic proton of which lies on a carbonyl group. Analogously, the downfield ethyl resonances appearing at δ 4.25 and 1.32 were assigned to the first $HCCCO_2Et$ ligand with its ethyl proton close to the CO ligand and the ethyl resonances at δ 3.21 and 0.30 are assigned to the second $HCCCO_2Et$ with its ethyl group lying on the phen ligand. These results are similar to those observed in complexes **2a,b**, and the ring-current effect is also employed to account for the great chemical-shift difference of the ethyl and acetylenic protons arising from different conformational arrangements. Because of the asymmetric nature of the tungsten center, the two methylene protons on the ethyl groups of **4b** produce AB-type coupling patterns at low temperatures. Most interestingly, the AB-type pattern remains in the fast-exchange limit. The latter observation is essential in determining the mechanism of alkyne rotation in these bis(alkyne) complexes. Similar dynamic NMR behavior is also observed for **4a**, **3a**, **3b**, and **3b′**. The ratios of conformers **A** to **B** are 4:1, 5:1, 4:1, and 5:1 for **4a,b** and **3a,b**, respectively.

The complex $W(CO)_2(4\text{-Mephen})(HCCCO_2Me)_2$ (**3b′**) deserves special attention due to the unsymmetric nature of the 4-Mephen ligand. The acetylenic protons of the major conformer **3b′-A**, being slightly different in environment, appear as a doublet at δ 9.38 at low temperature; two minor conformers **3b′-B′** and at **3b′-B″** in a 1:1 ratio were indicated by two doublets at δ 9.41 and 8.43 for the acetylenic protons and a signal at δ 2.74 for the methyl groups adjacent to the coordinated 4-Mephen. Resonances of the other two methyl groups close to the carbonyl groups appear at δ 3.75. The ratio of **3b′-A** to (**3b′-B′** + **3b′-B″**) is 5:1, close to the ratio of **3b-A** to **3b-B**. Above 223 K, isomer interconversion became faster and peak broadening was observed. The fast-exchange limit was reached at temperatures above 313 K. A doublet was still observed for the acetylenic protons in the fast-exchange limit.

Dynamic Behavior of $W(CO)_2(2\text{-}NH_2CH_2py)(DMAC)_2$ (1d) and $W(CO)_2(2\text{-}NH_2CH_2py)(PhCCCO_2Et)_2$ (2d). In ^1H NMR spectra of **1d** in the slow-exchange regime (below 193 K), four methyl resonances were observed due to the unsymmetric nature of

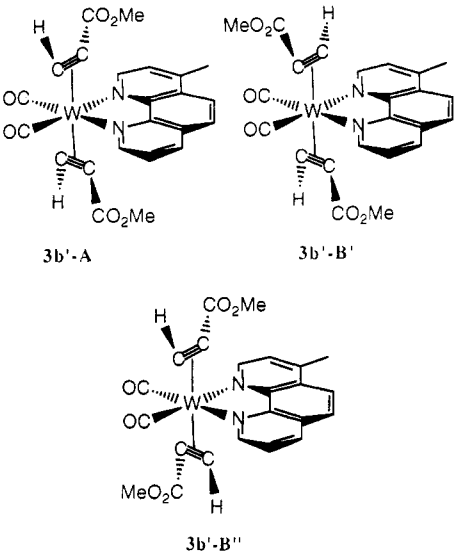

the $2\text{-}NH_2CH_2py$ ligand (Figure 3). The most upfield signal is assigned to the methyl group above the pyridyl ring, whereas the next signal corresponds to the methyl group close to the amino ligand. The methyl group near the carbonyl ligand opposite the pyridine ring is most downfield. In addition to the observation of varied chemical shifts for the methyl groups, the methylene and amino protons gave rise to two AB patterns in the the ^1H NMR spectrum at low temperatures. As the temperature was raised, the four methyl signals coalesced. Only one sharp single resonance at δ 3.65 was observed at 313 K. The two methylene protons of the chelating ligand became equivalent at this temperature. The proton signal of the amino group, owing to an overlapping methyl resonance, was not detected.

Figure 4 displays the ^1H NMR spectra of complex **2d** at various temperatures. The slow-exchange limit spectrum at 183 K is attributed to the presence of the two species **2d-A** and **2d-B**, geometrically related by 90°

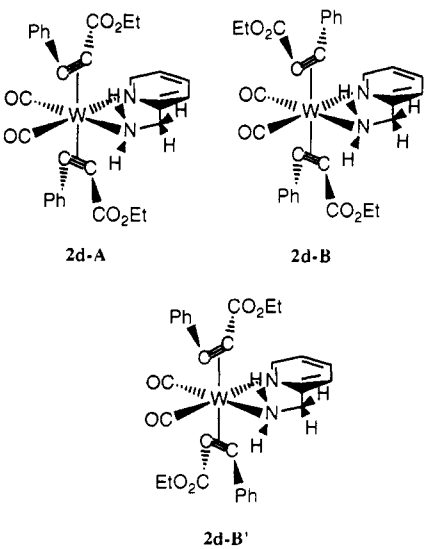

rotation of the acetylene ligands about the axis through the tungsten center and the centers of two carbon–carbon triple bonds. The major signals in the spectrum are assigned to the isomer **2d-A** on the basis of the results of X-ray structural analysis of complex **2a** and the fact that the ester group tends to stay adjacent to the nitrogen ligand

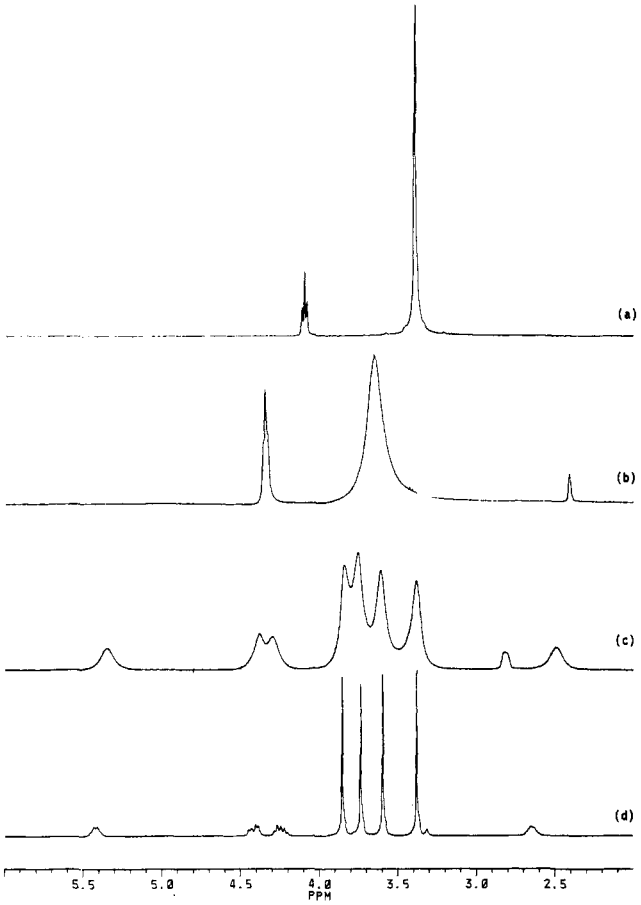

Figure 3. ^{1}H NMR spectra of $W(CO)_2(2\text{-}NH_2CH_2py)(DMAC)_2$ (**1d**) in $CDCl_3$ at various temperatures: (a) 313 K; (b) 293 K; (c) 263 K; (d) 243 K.

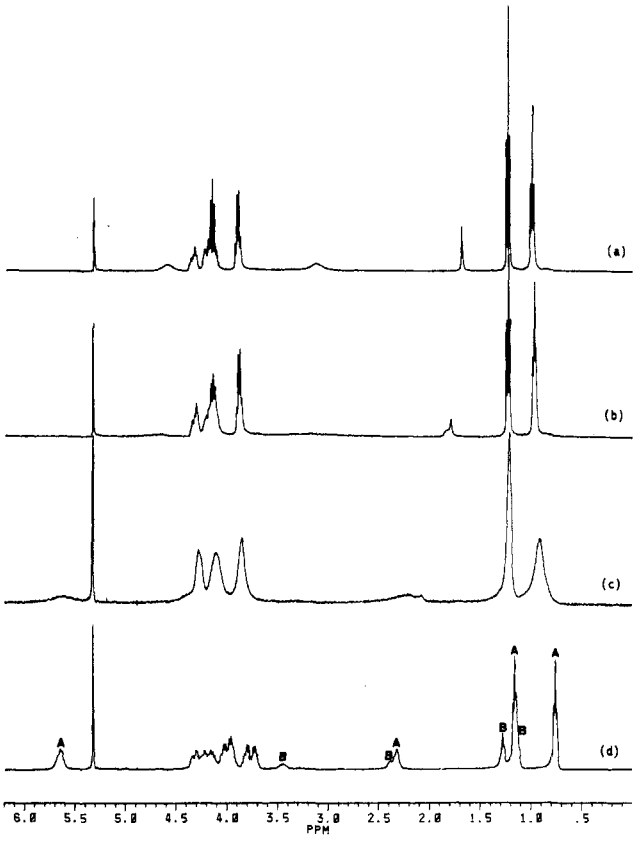

Figure 4. ^{1}H NMR spectra of $W(CO)_2(2\text{-}NH_2CH_2py)(PhCCCO_2Et)_2$ (**2d**) in CD_2Cl_2 at various temperatures: (a) 293 K; (b) 253 K; (c) 223 K; (d) 183 K.

to have better back-bonding. Only one ethyl group (at δ 0.71 and 3.73) in this structure is significantly affected by the ring current of the pyridyl group, in agreement with the proposed conformational arrangement in which one ester group lies on the pyridyl group. Complex **2d-B** is assigned to be the minor isomer, in view of the lack of ring current effect imparted by the pyridyl group for the two methyl resonances of $PhCCCO_2Et$ ligands at δ 1.14 (overlapping with one methyl resonance in **2d-A**) and 1.26. Among the possible conformational isomers for the minor species, **2d-B′** is excluded, because in this structure one ethyl group is right above the pyridyl ring and is expected to experience a substantial ring current effect. The assignment gains further support from the observation that there is only one rotational isomer, **A**, for the ethylenediamine complex **2c**; this result clearly indicates that as the $PhCCCO_2Et$ ligand lies on the N–W–CO vector in which N is an amino nitrogen, the direction of $PhCCCO_2Et$ with the ester group close to the amino group is strongly favored. Although the other possible conformer **2d-C**, in which both ester groups are directed to the carbonyl side, cannot be excluded on the basis of the observed chemical shift in the ^{1}H NMR spectrum, this conformational arrangement is highly unlikely according to consideration of the conformational preference and the orbital interactions in the complex. At temperatures above 203 K, interconversion of isomers **2d-A** and **2d-B** became fast and peak broadening was observed. Surprisingly, in the fast-exchange limit (above 273 K), two sets of ethyl signals remain in the ^{1}H NMR spectra (Figure 4). Moreover, the methylene protons on the ester groups and on 2-(aminomethyl)pyridine and the amino protons are all present as AB patterns in the fast-exchange regime and at the slow-exchange limit. These results indicate that the two acetylene ligands cannot interconvert and the complex enantiomers (e.g. **2d-A** and **2d-A***) do not racemize during the dynamic process.

Discussion

Each alkyne ligand in the present bis(alkyne) complexes **1–4** is considered as a two-electron donor from the electron count. The alkyne carbon resonances at 134–151 ppm in these complexes fall in th range of the predicted ^{13}C chemical shifts of a two-electron-donor alkyne, but the values are near the upper limit for these two-electron-donor ligands.[15] One major driving force for the observed ^{13}C data is the great electron-donating ability of the nitrogen ligands leading to strong back-donation from the metal center to the π^* orbitals of the alkyne ligands. Similarly, the observed ^{1}H NMR signals at ca. 9 ppm for the acetylenic protons of **3** and **4** appear to be remarkably downfield compared to the known two-electron-donor alkynes.[16] The stretching frequencies of the alkyne triple bonds in these complexes appear at ~1750 cm^{-1}, more than 400 cm^{-1} less than those of the free ligands and ca. 100–200 cm^{-1} less than that of $W(CO)_2(dppe)(DMAC)_2$.[2b] Consistent with the observed ^{13}C and ^{1}H NMR data, the present observed stretching frequencies are among the lowest ones for two-electron-donor acetylene complexes.[11a] For the same bidentate nitrogen ligand NN, the absorption

(15) Templeton, J. L.; Ward, B. C. *J. Am. Chem. Soc.* **1980**, *102*, 3288.
(16) Templeton, J. L.; Ward, B. C.; Chen, G. J.-J.; McDonald, J. W.; Newton, W. E. *Inorg. Chem.* **1981**, *20*, 1248.

frequencies of the carbonyl decrease in the order DMAC > $PhCCCO_2Et$ > $HCCCO_2Et \cong HCCCO_2Me$ (Table I). This trend may be understood on the basis of the π-acidities of these alkyne ligands, which decrease in the same order.

In the reactions of various alkynes with $W(CO)_3(NN)(CH_3CN)$, only electron-withdrawing alkynes gave stable bis(alkyne) complexes, indicating that the employment of strong π-acid alkynes to minimize the repulsion between filled d_π and $\pi_\perp$ orbitals of the alkynes are required. During the course of these reactions, no monocoordinated alkyne intermediate $W(CO)_3(NN)$(alkyne) was detected. The result suggests that once an alkyne is attached to the metal center, the carbonyl trans to the coordinated alkyne becomes labile and further substitution by another alkyne is rapid. Since alkynes do not react with $W(CO)_4(NN)$ at ambient temperature, we conclude that the present electron-withdrawing alkyne ligands have a greater trans effect than carbonyl groups.

One of the interesting features of the solid-state structure of **2a** is the unusual staggered and eclipsed conformation of the two trans alkyne ligands relative to one another and to a N–W–C vector, respectively. The eclipsed conformation is a sterically unfavorable arrangement, but this geometry minimizes the repulsion of the filled alkyne $\pi_\parallel$ and the filled metal d_{xy} orbitals and allows the interaction of the vacant alkyne $\pi_\perp$* with the filled metal d_{xy} orbitals, forming a δ bond.[17] Orthogonal and eclipsed conformations of trans π-acid ligands, including CO_2, O_2, and olefins, have been both observed and studied theoretically.[5-7]

A comparison of the bonding parameters of **2a** with those of the known complex $W(CO)_2(dppe)(DMAC)_2$ reveals a shorter average C≡C bond length (1.26 Å; cf. 1.30 Å), a larger average bend-back angle (142°; cf. 137°), and a shorter W–CO bond length (1.95 Å; cf. 2.03 Å) for **2a** relative to the dppe complex. Unlike the case for the NMR chemical shifts and stretching frequencies, there appears to be no clear trend for the bond distances and angles to reflect the donor–acceptor ability of ligands for these bis(alkyne) complexes. It is also interesting to compare the orientation of the ester groups of **2a** with those of other known bis(alkyne) complexes. In complex **2a**, the CO_2 carboxylate plane is perpendicular to the M–C_2 metal–alkyne plane (85.2°). In $W(CO)_2(dppe)(DMAC)_2$, the CO_2 carboxylate plane adjacent to the CO ligands is nearly parallel to the M–C_2 metal–alkyne plane (average angle 9°), whereas the carboxylate plane close to the phosphine ligands is considered perpendicular to the M–C_2 metal–alkyne plane (average angle 110°). On the other hand, in the molybdenum complex $Mo(CO)_2(bpy)(DMAC)_2$ all the CO_2 carboxylate planes tend to be perpendicular to the M–C_2 metal–alkyne planes (average angle 70°). Thus, in the more electron-donating systems (with bpy as ligand) or when the ester groups lie close to an electron-donor ligand (bpy and dppe) they tend to be perpendicular to the M–C_2 plane. Such an arrangement allows the overlap of the $\pi_\parallel$ orbitals (parallel to the M–C_2 plane) of the alkyne ligands with the p_π orbitals on the CO_2 carboxylate plane and increases the π-acidity of the alkyne ligands.

The observed directional selectivity of the $PhCCCO_2Et$ ligand is understood in terms of unsymmetric orbital overlap of the metal center with the alkyne ligands. An orbital interaction of the alkyne $\pi_\parallel$* and the tungsten d_π orbitals is illustrated in the diagram.

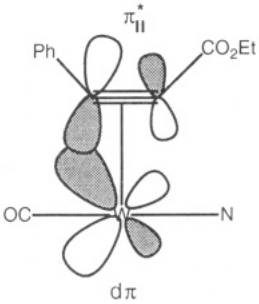

The metal d_π orbital is polarized as indicated in the diagram because of the great difference in electron-donating and -accepting ability of the bpy and carbonyl ligands. Thus, maximum overlap between the unsymmetric $\pi_\parallel$* orbital of the alkyne ligand and the d_π orbital of the metal center is only obtained when the $PhCCCO_2Et$ ligand eclipses an N–W–CO vector with the phenyl end adjacent to the carbonyl ligand.

Mechanism of Alkyne Rotation. Under the conditions for dynamic NMR investigations, there is no ligand exchange observed between external alkynes and the coordinated alkyne ligands. Thus, an intermolecular process involving dissociation–association of alkynes is ruled out for the dynamic behavior of complexes **1–4**. To account for the dynamic NMR behavior of the present bis(alkyne) complexes, there are three different possible intramolecular processes: (i) disrotatory motion of the two coordinated alkynes; (ii) independent rotation of the alkyne ligands; (iii) conrotatory motion of the two coordinated alkynes. In the following, these processes are carefully considered in order to determine the correct mechanism for the alkyne rotation.

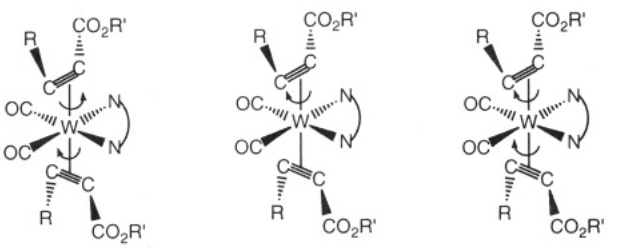

Disrotation of two alkyne ligands in complexes **2–4** accounts for the interconversion of the corresponding rotamers **A** and **C** (Scheme I; complex **2a** taken as a representative example). However, this mechanism fails to explain the facile interconversion of **A**, **B**, and **C** observed in the variable-temperature ^1H NMR spectra of complex **2a**. Moreover, the pathway allows the interconversion of enantiomers **A** and **A***, **B** and **B***, etc. The observation of an AB pattern for the methylene protons of the $HCCCO_2Et$ ligands in complex **4b** and the 2-NH_2CH_2py ligands in complex **2d** in the ^1H NMR spectra even at the fast-exchange limit (Figure 4) clearly stands against this proposed mechanism; the two methylene protons would undergo exchange to give a simple quartet (coupling from the methyl group) in the fast-exchange limit if the enantiomeric structures **A** and **A*** and **B** and **B*** are allowed to interchange.

Mechanism ii assumes an independent rotation by 180° of one alkyne ligand with the other remaining at the same conformation. Application of this mechanism to the present bis(alkyne) complexes with symmetric bidentate

(17) Albright, T. A.; Hoffmann, R.; Thibeault, J. C.; Thorn, D. L. *J. Am. Chem. Soc.* **1979**, *101*, 3801.

Scheme I. Disrotatory Motion of the Alkynes in 2a[a,b]

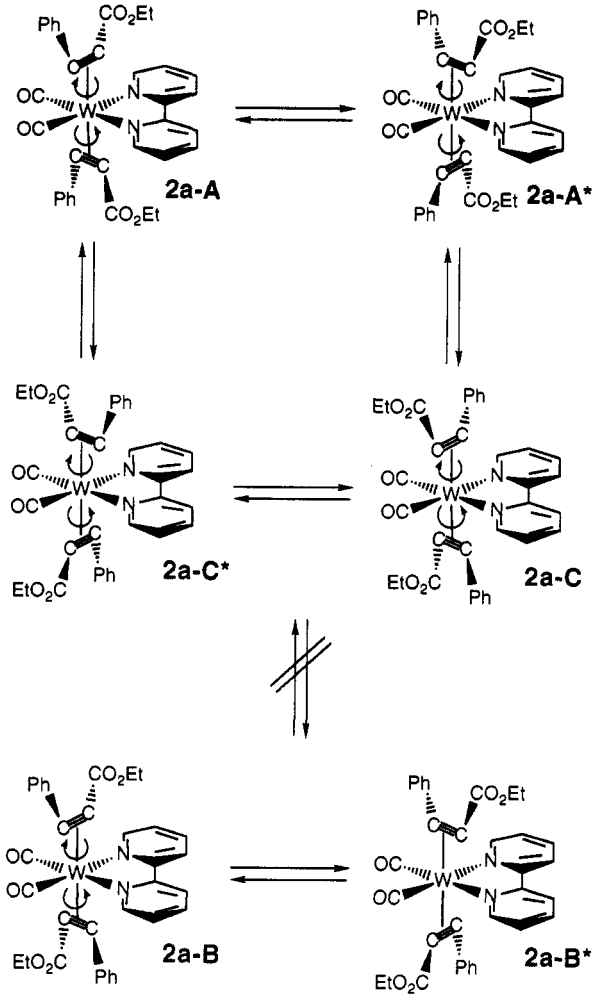

[a] The asterisks denote enantiomeric structures.[b] The arrows indicated in the structures are for clockwise transformation.

nitrogen ligands, e.g. **1a**, **2a**, and **3a**, successfully accounts for interconversion of the observed rotational isomers. Furthermore, the enantiomeric structures do not interchange for all bis(alkyne) complexes, consistent with the observations of variable-temperature NMR spectra. However, this mechanism fails to explain the equivalency of the four methyl groups in the two DMAC ligands of complex **1d** (Figure 3) in the fast-exchange limit and can therefore be discarded on this basis.

Another independent rotation of alkyne ligands (mechanism ii') involves the rotation of a coordinated alkyne by 90° to give intermediates such as I, followed by an independent rotation of one alkyne by 90°. A detailed

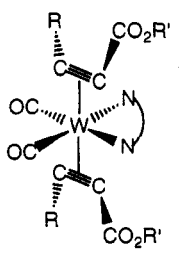

I

analysis of this mechanism indicated that this rotational process leads to fluxional behavior equivalent to that from

Scheme II. Conrotatory Motion of the Alkynes in 2d[a]

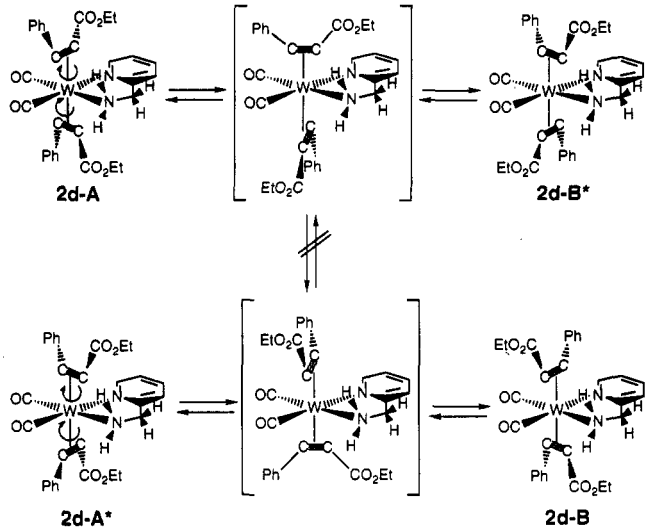

[a] The asterisks denote enantiomeric structures.

a combination of mechanism i and ii. This mechanism predicts a single resonance for the methyl and methylene protons on the PhCCCOOEt ligands of complex **2d**. The application of the mechanism to the bis(alkyne) complexes indicates the interchange of enantiomeric structures in the fast-exchange limit. These features are clearly contrary to the results of the variable-temperature spectra of compound **2d**. On this basis, the mechanism can be disregarded.

Finally, the mechanism of conrotatory motion of the alkyne ligands is left to be considered. According to this process, the two trans alkynes rotate synchronously in the same direction and thus remain mutually orthogonal during the rotation. A transition state or an intermediate such as II is expected to be involved in this intramolecular

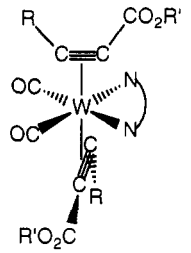

II

process. It appears to be the only mechanism that can fit all experimental facts for complexes **1–4**. As shown in Scheme II, the process successfully explains the interconversion of the rotational isomers **2d-A** and **2d-B**. In agreement with the existence of AB patterns for the methylene protons both on the alkyne ligands and on the 2-NH_2CH_2py ligand in the NMR spectra even in the fast-exchange regime, the rotation leads to no interchange of enantiomeric structures. Moreover, this conrotatory motion of the alkyne ligands accounts for the observation of two nonequivalent ethyl groups and phenyl groups of the $PhCCCO_2Et$ ligands in the ^1H NMR spectrum in the fast-exchange regime. Application of the mechanism to the rotation of alkynes in complex **1d** indicates that the observed four methyl resonances of the DMAC ligands in the slow-exchange limit would average to a single resonance in the fast-exchange limit as we observed. The intercon-

version of the three rotational isomers **A–C** of complex **2a** (Scheme III) and **2b** and the observation of both two nonequivalent acetylene protons of complex **3b′** and an AB type pattern for the two methylene protons of **4b** in the fast-exchange regime also may be rationalized according to this mechanism. Therefore, we conclude that the observed dynamic NMR behavior of these bis(alkyne) complexes results from the conrotatory motion of the alkyne ligands.

In conclusion, we have achieved the synthesis of tungsten(0) complexes having a bidentate nitrogen ligand and two trans alkynes. In solution, the complexes with unsymmetric alkynes exist as a mixture of conformational isomers arising from the directional selectivity of the unsymmetric alkyne ligands relative to the N–W–CO vectors. According to their variable-temperature NMR spectra these conformational isomers undergo rapid interconversion at ambient temperature but become static at low temperatures (ca. 200 K). The conformational structures and their relative ratios have been determined from the NMR spectra at temperatures in the slow-exchange limit. Stable terminal bis(propiolate) complexes (**3** and **4**) were also prepared;[18] they have unusual downfield chemical shifts for the acetylenic protons and are among the few terminal alkyne d^6 complexes[2b] that do not undergo rearrangement to the corresponding vinylidene species.[19] Of the possible mechanisms proposed for the dynamic NMR behavior of these trans bis(alkyne) complexes, only the process of conrotatory motion of the two alkyne ligands in which both ligands rotate synchronously in the same direction accounts for all observations.

Experimental Section

All reactions were performed under dry nitrogen, and all solvents were dried by standard methods. The ^1H and ^{13}C NMR spectra were recorded on a Bruker AM-400 instrument; infrared spectra were measured on a Bomem MB-100 spectrometer. Structural determination was carried out on a Siemens R3m/V diffractometer.

Dimethyl acetylenedicarboxylate and ethylenediamine (Merck), methyl propiolate, ethyl propiolate, ethyl phenylpropiolate, 2-(aminomethyl)pyridine, 2,2′-bipyridine, 1,10-phenanthroline, and 4-methyl-1,10-phenanthroline (Aldrich), and tungsten hexacarbonyl (Janssen) were used as received. Tris(acetonitrile)tricarbonyltungsten was prepared according to a reported method.[20]

Synthesis of $W(CO)_2$(phen)(DMAC)$_2$ (1b). A 100-mL side-arm flask containing $W(CO)_3(CH_3CN)_3$ (0.500 g, 1.28 mmol) and 1,10-phenanthroline (0.230 g, 1.28 mmol) was evacuated and purged with nitrogen gas three times. Acetonitrile (20 mL) was added to the system, and the solution was stirred for 30 min; the solution became purple during this period. DMAC (dimethyl acetylenedicarboxylate; 0.360 mL, 2.94 mmol) was then added to the solution, and the solution was stirred for another 12 h. The solution was concentrated and separated on a silica gel column using dichloromethane as eluent to afford a crude yellow solid. Recrystallization from a mixture of dichloromethane and hexane gave the desired pure product (0.52 g) in 62% yield. ^1H NMR (400 MHz, $CDCl_3$, 20 °C): δ 3.42 (br s, CH_3, 12 H), 7.78 (dd, J = 8.1 Hz, J = 4.3 Hz, H-3,8 of phen, 2 H), 7.95 (s, H-5,6 of phen, 2 H), 8.49 (d, J = 8.1 Hz, H-4,7 of phen, 2 H), 9.28 (d, J = 4.3 Hz, H-2,9 of phen, 2 H). ^{13}C NMR (100 MHz, $CDCl_3$, 20 °C): δ 51.32 (CH_3), 124.54, 126.73, 130.11, 137.89, 145.98, 152.37, 169.85 (COO), 212.53 (C≡O). IR (KBr): 2013 (s) (ν(C≡O), 1945 (s), (ν(C≡O)), 1769 (b) (ν(C≡C)), 1687 (m) (ν(COO)) cm^{-1}. MS (FAB): m/z 704 (M^+), 648 ($M^+ - 2$ CO), 562 (M^+ – DMAC); Anal. Calcd for $WC_{26}H_{20}N_2O_{10}$: C, 44.34; H, 2.86; N, 3.98. Found: C, 44.25; H, 2.85; N, 4.00.

Scheme III. Conrotatory Motion of the Alkynes in 2a[a]

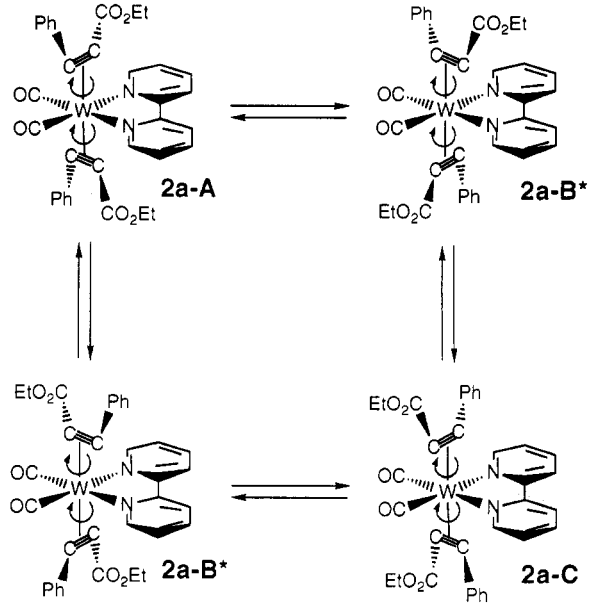

[a] The arrows indicated in the structures are for clockwise transformation.

The tungsten bis(alkyne) complexes indicated in eq 1 were thus prepared in 20–60% yield. The yields of these complexes, important spectral data, and analytical data are summarized as follows.

$W(CO)_2$(bpy)(DMAC)$_2$ (1a): ^1H NMR (400 MHz, $CDCl_3$, 20 °C) δ 3.52 (br s, CH_3, 12 H), 7.40 (dd, J = 5.2 Hz, J = 4.6 Hz, H-4,4′ of bpy, 2 H), 7.96 (dd, J = 8.2 Hz, J = 4.6 Hz, H-5,5′ of bpy, 2 H), 8.19 (d, J = 8.2 Hz, H-6,6′ of bpy, 2 H), 8.81 (d, J = 5.2 Hz, H-3,3′ of bpy, 2 H); ^{13}C NMR (100 MHz, $CDCl_3$, 20 °C) δ 51.69 (CH_3), 121.93, 126.55, 138.49, 152.97, 154.29, 179.12 (COO), 211.97 (C≡O); IR (KBr) 2010 (s) (ν(C≡O)), 1940 (s) (ν(C≡O)), 1775 (b) (ν(C≡C)), 1695 (m) (ν(COO)) cm^{-1}; MS (FAB) m/z 680 (M^+), 624 ($M^+ - 2$ CO), 538 (M^+ – DMAC). Anal. Calcd for $WC_{24}H_{20}N_2O_{10}$: C, 42.37; H, 2.96; N, 4.12. Found: C, 42.25; H, 3.00; N, 4.11.

$W(CO)_2$(bpy)(PhCCCO$_2$Et)$_2$ (2a): ^1H NMR (400 MHz, $CDCl_3$, 20 °C) δ 1.01 (br s, CH_3, 6 H), 3.89 (br s, CH_2, 4 H), 7.14–7.22 (m, Ph, 10 H), 7.36 (dd, J = 5.4 Hz, J = 4.7 Hz, H-4,4′ of bpy, 2 H), 7.89 (dd, J = 8.1 Hz, J = 4.7 Hz, H-5,5′ of bpy, 2 H), 7.94 (d, J = 8.1 Hz, H-6,6′ of bpy, 2 H), 8.87 (d, J = 5.4 Hz, H-3,3′ of bpy, 2 H); ^{13}C NMR (100 MHz, CD_2Cl_2, 20 °C) δ 14.37 (CH_3), 60.26 (CH_2), 122.49, 126.78, 127.30, 128.56, 128.78, 138.14, 138.50, 153.07, 154.50, 172.31 (COO), 218.00 (C≡O); IR (KBr) 1988 (s) (ν(C≡O)), 1915 (s) (ν(C≡O)), 1739 (b) (ν(C≡C)), 1671 (m) (ν(COO)) cm^{-1}; MS (FAB) m/z 745 (M^+ + 1), 688 ($M^+ - 2$ CO), 570 ($M^+ - C_{11}H_{10}O_2$). Anal. Calcd for $WC_{34}H_{28}O_6N_2$: C, 54.86; H, 3.79; N, 3.76. Found: C, 54.47; H, 3.80; N, 3.73.

$W(CO)_2$(phen)(PhCCCO$_2$Et)$_2$ (2b): ^1H NMR (400 MHz, CD_2Cl_2, 20 °C) δ 0.82 (br s, CH_3, 6 H), 3.72 (br s, CH_2, 4 H), 7.18–7.29 (m, Ph, 10 H), 7.75 (dd, J = 8.1 Hz, J = 4.7 Hz, H-3,8 of phen, 2 H), 7.91 (s, H-5,6 of phen, 2 H), 8.45 (d, J = 8.1 Hz, H-4,7 of phen, 2 H), 9.22 (d, J = 4.7 Hz, H-2,9 of phen, 2 H); ^{13}C NMR (100 MHz, CD_2Cl_2, 20 °C) δ 13.05 (CH_3), 58.82 (CH_2), 124.33, 125.93, 126.34, 127.04, 127.38, 129.17, 136.13, 136.95, 144.77, 151.10, 170.02 (COO), 216.49 (C≡O); IR (KBr) 1984 (s) (ν(C≡O)), 1909 (s) (ν(C≡O)), 1736 (b) (ν(C≡C)), 1672 (m) (ν(COO)); MS

(18) Buang, N. A.; Hughes, D. L.; Kashef, N.; Pichards, R. L.; Pombeiro, A. L. *J. Organomet. Chem.* **1987**, *323*, C47.
(19) (a) Silvestre, J.; Hoffmann, R. *Helv. Chim. Acta* **1985**, *68*, 1461. (b) Bianchini, C.; Peruzzini, M.; Vacca, A.; Zanobini, F. *Organometallics* **1991**, *10*, 3697. (c) Bulock, R. M. *J. Chem. Soc., Chem. Commun.* **1989**, 165. (d) Bruce, M. I.; Swincer, A. G. *Adv. Organomet. Chem.* **1983**, *22*, 59. (e) Bitcon, C.; Whiteley, M. W. *J. Organomet. Chem.* **1987**, *336*, 385. (f) Birdwhistell, K. R.; Burgmayer, S. J. N.; Templeton, J. L. *J. Am. Chem. Soc.* **1983**, *105*, 7789.
(20) Tate, D. P.; Knipple, W. R.; Augl, J. M. *Inorg. Chem.* **1962**, *1*, 433.

(FAB) m/z 769 ($M^+ + 1$), 712 ($M^+ - 2$ CO), 594 ($M^+ - C_{11}H_{10}O_2$). Anal. Calcd for $WC_{36}H_{28}N_2O_6$: C, 56.29; H, 3.67; N, 3.65. Found: C, 54.80; H, 3.67; N, 3.60.

$W(CO)_2$(4-Mephen)($PhCCCO_2Et$)$_2$ (2b′): ^{1}H NMR (400 MHz, CD_2Cl_2, 20 °C) δ 0.73 (br s, CH_3, 6 H), 2.84 (s, CH_3, 3H), 3.63 (br s, CH_2, 4 H), 7.13–7.25 (m, Ph, 10 H), 7.58 (d, J = 5.1 Hz, H-3 of phen, 1 H), 7.72 (dd, J = 8.1 Hz, J = 4.9 Hz, H-8 of phen, 1 H) [7.93, 8.07 (d, J = 8.9 Hz, H-5,6 of phen, 2 H)], 8.44 (d, J = 8.1 Hz, H-7 of phen, 1 H), 9.03 (d, J = 5.1 Hz, H-2 of phen, 1 H), 9.16 (d, J = 4.9 Hz, H-9 of phen, 1 H); ^{13}C NMR (100 MHz, CD_2Cl_2, 20 °C) δ 13.97 (CH_3), 19.01 (CH_3), 59.68 (CH_2), 123.64, 125.02, 126.11, 126.74, 127.93, 128.22, 129.67, 136.91, 137.86, 145.32, 145.91, 146.96, 151.45, 152.02, 171.06 (COO), 217.41 (C≡O); IR (KBr) 1982 (s) (ν(C≡O)), 1908 (s) (ν(C≡O)), 1736 (b) (ν(C≡C)), 1671 (m) (ν(COO)); MS (FAB) m/z 783 ($M^+ + 1$), 726 ($M^+ - 2$ CO), 608 ($M^+ - C_{11}H_{10}O_2$). Anal. Calcd for $WC_{37}H_{30}N_2O_6$: C, 56.79; H, 3.86; N, 3.58. Found: C, 57.03; H, 3.74; N, 3.63.

$W(CO)_2$(bpy)($HCCCO_2Me$)$_2$ (3a): ^{1}H NMR (400 MHz, CD_2Cl_2, 20 °C) δ 3.19 (s, CH_3, 6 H), 7.58 (dd, J = 5.9 Hz, J = 4.5 Hz, H-4,4′ of bpy, 2 H), 8.17 (dd, J = 8.4 Hz, J = 4.5 Hz, H-5,5′ of bpy, 2 H), 8.49 (d, J = 8.4 Hz, H-6,6′ of bpy, 2 H), 8.69 (d, J = 5.9 Hz, H-3,3′ of bpy, 2 H), 9.20 (s, ≡C—H, 1 H); ^{13}C NMR (100 MHz, CD_2Cl_2, 20 °C) δ 51.17 (CH_3), 122.35, 126.64, 136.32 (≡C—H), 138.48, 141.40 (≡C—R), 152.73, 154.63, 170.91 (COO), 218 77 (C≡O); IR (KBr) 1978 (s) (ν(C≡O)), 1901 (s) (ν(C≡O)), 1724 (b) (ν(C≡C)), 1661 (m) (ν(COO)) cm^{-1}; MS (FAB) m/z 565 ($M^+ + 1$), 508 ($M^+ - 2$ CO), 480 ($M^+ - C_4H_4O_2$). Anal. Calcd for $WC_{20}H_{16}O_6N_2$: C, 42.58; H, 2.86; N, 4.97. Found: C, 42.20; H, 3.02; N, 4.67.

$W(CO)_2$(phen)($HCCCO_2Me$)$_2$ (3b): ^{1}H NMR (400 MHz, CD_2Cl_2, 20 °C) δ 3.06 (s, CH_3, 6 H), 7.78 (dd, J = 8.2 Hz, J = 5.0 Hz, H-3,8 of phen, 2 H), 8.02 (s, H-5,6 of phen, 2 H), 8.53 (d, J = 8.2 Hz, H-4,7 of phen, 2 H), 9.06 (d, J = 5.0 Hz, H-2,9 of phen, 2 H), 9.39 (s, ≡C—H, 2 H); ^{13}C NMR (100 MHz, CD_2Cl_2, 20 °C) δ 50.79 (CH_3), 125.08, 127.27, 129.87, 134.95 (≡C—H), 136.84, 143.76 (≡C—R), 145.93, 151.95, 171.92 (COO), 217.71 (C≡O); IR (KBr) 1973 (s) (ν(C≡O)), 1896 (s) (ν(C≡O)), 1723 (b) (ν(C≡C)), 1661 (m) (ν(COO)); MS (FAB) m/z 589 ($M^+ + 1$), 532 ($M^+ - 2$ CO), 504 ($M^+ - C_4H_4O_2$). Anal. Calcd for $WC_{22}H_{16}N_2O_6$: C, 44.92; H, 2.74; N, 4.76. Found: C, 43.86; H, 2.85; N, 4.72.

$W(CO)_2$(4-Mephen)($HCCCO_2Me$)$_2$ (3b′): ^{1}H NMR (400 MHz, CD_2Cl_2, 20 °C) δ 2.87 (s, CH_3, 3 H), 3.01 (br s, CH_3, 6 H), 7.55 (d, J = 5.2 Hz, H-3 of phen, 1 H), 7.71 (dd, J = 8.2 Hz, J = 4.8 Hz, H-8 of phen, 1 H), [7.98, 8.12 (d, J = 9.0 Hz, H-5,6 of phen, 2 H)], 8.47 (dd, J = 8.2 Hz, J = 1.4 Hz, H-7 of phen, 1 H), 8.84 (d, J = 5.2 Hz, H-2 of phen, 1 H), 8.98 (dd, J = 4.8 Hz, J = 1.4 Hz, H-9 of phen, 1 H), 9.39 (br s, ≡C—H, 2 H); ^{13}C NMR (100 MHz, CD_2Cl_2, 20 °C) δ 18.96 (CH_3), 50.72 (CH_3), 123.72, 124.94, 126.07, 126.77, 129.66, 136.88, 145.50, 146.12, 146.98, 151.28, 151.86, 171.30 (COO), 218.04, 218.19 (C≡O); IR (KBr) 1974 (s) (ν(C≡O)), 1898 (s) (ν(C≡O)), 1718 (b) (ν(C≡C)), 1661 (m) (ν(COO)); MS (FAB) m/e 603 ($M^+ + 1$), 546 ($M^+ - 2$CO), 518 ($M^+ - C_4H_4O_2$). Anal. Calcd for $WC_{23}H_{18}N_2O_6$: C, 45.87; H, 3.01; N, 4.65. Found: C, 45.23; H, 3.16; N, 4.77.

$W(CO)_2$(bpy)($HCCCO_2Et$)$_2$ (4a): ^{1}H NMR (400 MHz, CD_2Cl_2, 20 °C) δ 0.86 (t, J = 7.0 Hz, CH_3, 6 H), 3.68 (q, J = 7.0 Hz, CH_2, 4 H), 7.38 (dd, J = 5.2 Hz, J = 4.6 Hz, H-4,4′ of bpy, 2 H), 7.96 (dd, J = 8.1 Hz, J = 4.6 Hz, H-5,5′ of bpy, 2 H), 8.08 (d, J = 8.1 Hz, H-6,6′ of bpy, 2 H), 8.66 (d, J = 5.2 Hz, H-3,3′ of bpy, 2 H), 9.25 (s, ≡C—H, 1 H); ^{13}C NMR (100 MHz, CD_2Cl_2, 20 °C) δ 13.39 (CH_3), 59.10 (CH_2), 121.21, 125.54, 134.07 (≡C—H), 137.32, 141.40 (≡C—R), 151.42, 153.37, 170.61 (COO), 217.47 (C≡O); IR (KBr) 1976 (s) (ν(C≡O)), 1899 (s) (ν(C≡O)), 1721 (b) (ν(C≡C)), 1659 (m) (ν(COO)); MS (FAB) m/z 593 ($M^+ + 1$), 536 ($M^+ - 2$ CO), 494 ($M^+ - C_5H_6O_2$). Anal. Calcd for $WC_{22}H_{20}N_2O_6$: C, 42.58; H, 2.86; N, 4.97. Found: C, 42.20; H, 2.92; N, 4.77.

$W(CO)_2$(phen)($HCCCO_2Et$)$_2$ (4b): ^{1}H NMR (400 MHz, CD_2Cl_2, 20 °C) δ 0.63 (br s, CH_3, 6 H), 3.48 (br s, CH_2, 4 H), 7.77 (dd, J = 8.1 Hz, J = 4.0 Hz, H-3,8 of phen, 2 H), 8.02 (s, H-5,6 of phen, 2 H), 8.52 (d, J = 8.1 Hz, H-4,7 of phen, 2 H), 8.54 (d, J = 4.0 Hz, H-2,9 of phen, 2 H), 9.38 (s, ≡C—H, 2 H); ^{13}C NMR (100 MHz, 20 °C) δ 13.78 (CH_3), 59.20 (CH_2), 125.16, 127.23, 129.21, 134.27 (≡C—H), 136.97, 142.67 (≡C—R), 145.71, 151.71, 171.02 (COO), 218.04 (C≡O); IR (KBr) 1977 (s) (ν(C≡O)), 1719 (b) (ν(C≡C)), 1660 (m) (ν(COO)); MS (FAB) m/z 617 ($M^+ + 1$), 560 ($M^+ - 2$ CO), 518 ($M^+ - C_5H_6O_2$). Anal. Calcd for $WC_{24}H_{20}N_2O_6$: C, 46.77; H, 3.27; N, 4.55. Found: C, 45.97; H, 3.26; N, 4.50.

Synthesis of $W(CO)_2$(en)($DMAC$)$_2$ (1c). A 100-mL side-arm flask containing $W(CO)_3(CH_3CN)_3$ (0.500 g, 1.28 mmol) was evacuated and purged with nitrogen gas three times. Ethylenediamine (0.077 g, 1.28 mmol) and acetonitrile (20 mL) were added to the system, and the solution was stirred for 30 min; the solution gradually became yellow during the reaction. To the system was added DMAC (0.360 mL, 2.94 mmol), and the solution was stirred for another 12 h; a stream of nitrogen gas was passed through the flask to remove the carbon monoxide. The resulting mixture was concentrated and separated on a silica gel column using a mixture (5:1 by volume) of dichloromethane and acetone as eluent to afford a crude yellow solid. Recrystallization from a mixture of dichloromethane and hexane gave the desired pure product (0.18 g) in 24% yield. ^{1}H NMR (400 MHz, $CDCl_3$, 20 °C): δ 2.67 (br s, CH_2, 4 H), 3.80 (s, CH_3, 12 H). ^{13}C NMR (100 MHz, $CDCl_3$, 20 °C): δ 42.57 (CH_2), 53.86 (CH_3), 209.14 (C≡O). IR (KBr): 2011 (s) (ν(C≡O)), 1937 (s) (ν(C≡O)), 1741 (b) (ν(C≡C)), 1684 (m) (ν(COO)) cm^{-1}. MS (FAB): m/z 583 ($M^+ + 1$), 526 ($M^+ - 2$ CO), 496 (M^+ - DMAC). Anal. Calcd for $WC_{16}H_{20}N_2O_{10}$: C, 32.90; H, 3.45; N, 4.80. Found: C, 33.16; H, 3.51; N, 4.92.

By a similar procedure $W(CO)_2$(en)($PhCCCO_2Et$)$_2$ (**2c**) and $W(CO)_2$(2-CH_2NH_2py)($DMAC$)$_2$ (**1d**) were obtained in 15% and 51% yields, respectively.

$W(CO)_2$(2-NH_2CH_2py)($DMAC$)$_2$ (1d): ^{1}H NMR (400 MHz, $CDCl_3$, 20 °C) δ 3.65 (br s, CH_3, 12 H), 4.34 (br m, CH_2, 2 H), 7.14 (m, H-3,5 of py, 2 H), 7.67 (m, H-4 of py, 1 H), 8.41 (d, J = 5.4 Hz, H-6 of py, 1 H); ^{13}C NMR (100 MHz, $CDCl_3$, 20 °C) δ 49.56 (CH_2), 52.06 (CH_3), 120.66, 124.11, 138.17, 151.73, 158.99, 210.20 (C≡O), 210.65 (C≡O); IR (KBr) 2011 (s) (ν(C≡O)), 1938 (s) (ν(C≡O)), 1746 (b) (ν(C≡C)), 1689 (m) (ν(COO)) cm^{-1}; MS (FAB) m/z 632 (M^+), 576 ($M^+ - 2$ CO), 490 (M^+ - DMAC). Anal. Calcd for $WC_{20}H_{20}N_2O_{10}$: C, 38.00; H, 3.19; N, 4.43. Found: C, 37.90; H, 3.17; N, 4.50.

$W(CO)_2$(en)($PhCCCO_2Et$)$_2$ (2c): ^{1}H NMR (400 MHz, CD_2Cl_2, 20 °C) δ 1.39 (t, J = 7.1, CH_3, 6 H), 1.82 (br s, NH_2, 2H), 2.48 (br s, CH_2, 2 H), 2.93 (br s, CH_2, 2 H), 4.31 (m, OCH_2, 4 H), 7.28–7.65 (m, Ph, 10 H); ^{13}C NMR (100 MHz, CD_2Cl_2, 20 °C) δ 14.20 (CH_3), 42.32 (CH_2), 60.65 (OCH_2), 127.73, 128.49, 129.05, 137.63 (C≡C), 139.79 (C≡C), 159.42, 170.04 (COO), 215.57 (C≡O); IR (KBr) 1981 (s) (ν(C≡O)), 1907 (s) (ν(C≡O)), 1725 (b) (ν(C≡C)), 1660 (m) (ν(COO)) cm^{-1}; MS (FAB) m/z 649 ($M^+ + 1$), 592 ($M^+ - 2$ CO), 474 ($M^+ - C_{11}H_{10}O_2$). Anal. Calcd for $WC_{26}H_{28}N_2O_6$: C, 48.17; H, 4.35; N, 4.32. Found: C, 47.98; H, 4.35; N, 4.42.

Synthesis of $W(CO)_2$[2-(NH_2CH_2)py]($PhCCCO_2Et$)$_2$ (2d). A 100-mL side-arm flask containing $W(CO)_3(CH_3CN)_3$ (0.500 g, 1.28 mmol) was evacuated and purged with nitrogen gas three times. To the system, were added 4-methylpyridine (0.24 g, 2.56 mmol) and acetonitrile (20 mL), and the resulting solution was stirred for 2 h. The solution color gradually changed to purple during the reaction. Ethyl phenylpropiolate (0.52 mL, 3.07 mmol) was then added to the solution, and the mixture was stirred for another 12 h, leading to the precipitation of a brown solid of $W(CO)_2$(4-Mepy)$_2$($PhCCCO_2Et$)$_2$ (0.44 g). ^{1}H NMR (400 MHz, $CDCl_3$, 20 °C): δ 1.19 (t, J = 7.1 Hz, CH_3, 6 H), 2.34 (s, CH_3, 6 H), 4.12 (m, CH_2, 4 H), 7.03 (br s, H-3,5 of py, 4 H), 7.04–7.27 (m, Ph, 10 H), 8.47 (br s, H-2,6 of py, 4 H). IR (KBr): 1983 (s) (ν(C≡O)), 1910 (s) (ν(C≡O)), 1733 (b) (ν(C≡C)), 1673 (m) (ν(COO)) cm^{-1}. A stream of nitrogen gas was passed through the flask to remove the carbon monoxide produced during this period. The precipitate (0.44 g) and 2-(aminomethyl)pyridine (0.070 g) were then dissolved in 15 mL of acetonitrile, and this solution was stirred at ambient temperature for 10 min. The solvent was evaporated, and the remaining solid was recrystallized from a dichloromethane and n-hexane mixture to give the desired yellow

Table III. Summary of Crystal Data Collection for 2a

empirical formula	$C_{34}H_{28}N_2O_6W$
color; habit	orange; needle
cryst size, mm³	0.03 × 0.05 × 0.20
space group	monoclinic; *Cc*
unit cell dimensions	
a, Å	15.523(5)
b, Å	9.676(2)
c, Å	21.471(6)
β, deg	108.17(2)
volume, Å³	3064.4(13)
Z	4
formula weight	744.4
density (calc), g cm⁻³	1.614
abs coeff, cm⁻¹	3.895
F(000)	1472
temp, K	296
2*θ* range, deg	2.5–50.0
scan type	*θ*/2*θ*
scan speed, deg min⁻¹	variable; 2.93–14.65 in *ω*
scan range (*ω*), deg	1.00 plus Kα separation
index ranges	$0 \le h \le 18, 0 \le k \le 11, -25 \le l \le 21$
no. of reflns collected	3153 (1711 > 3.0*σ*(*I*))
no. of indep rflns	2810 (1682 > 3.0*σ*(*I*))
final *R* indices (obs data)	$R = 0.0352$, $R_w = 0.0349$
goodness of fit	1.21
largest and mean Δ/*σ*	0.006, 0.001
data-to-param ratio	9.5:1
largest diff peak/hole, e Å⁻³	+1.05/−0.51

crystalline product (0.40 g) in 44% yield. ^{1}H NMR (400 MHz, CD_2Cl_2, 20 °C): δ 1.03 (t, *J* = 7.1 Hz, CH_3, 3 H), 1.25 (t, *J* = 7.1 Hz, CH_3, 3 H), 3.12 (br, NH_2, 1 H), 3.93 (q, *J* = 7.1 Hz, OCH_2, 2 H), 4.12 (m, OCH_2, 2 H), 4.20–4.37 (m, CH_2, 2 H), 4.50 (br, NH_2, 1 H), 7.13 (m, H-3,5 of py, 2 H), 7.21–7.51 (m, Ph, 10 H), 7.69 (m, H-4 of py, 1 H), 8.40 (d, *J* = 5.4 Hz, H-6 of py, 1 H). ^{13}C NMR (100 MHz, CD_2Cl_2, 20 °C): δ 14.30 (CH_3), 14.38 (CH_3), 49.66 (CH_2), 60.30 (OCH_2), 60.73 (OCH_2), 121.06, 124.13, 127.33, 128.49, 128.58, 128.68, 137.69, 138.10, 139.89, 142.97, 151.27, 151.76, 157.07, 159.36, 170.31 (COO), 171.68 (COO), 215.95 (C≡O), 217.01 (C≡O). IR (KBr): 1982 (s) (*ν*(C≡O)), 1908 (s) (*ν*(C≡O)), 1727 (b) (*ν*(C≡C)), 1669 (m) (*ν*(COO)) cm⁻¹. MS (FAB): *m*/*z* 697 (M^+ + 1), 640 (M^+ − 2 CO), 522 ($M^+ - C_{11}H_{10}O_2$). Anal. Calcd for $WC_{30}H_{28}N_2O_6$: C, 51.74; H, 4.05; N, 4.02. Found: C, 51.48; H, 4.01; N, 4.12.

X-ray Structure Determination of W(bpy)(CO)$_2$(PhCCCO$_2$Et)$_2$ (2a). An orange crystal of dimensions 0.03 × 0.05 × 0.20 mm³ was selected for X-ray diffraction. Diffraction data were collected on a Siemens R3m/V diffractometer equipped with a graphite-monochromated Mo source (Kα radiation, 0.7107 Å). Cell parameters as listed in Table III were determined from the fit of 18 reflections ($7.14 \le 2\theta \le 21.95°$). The other parameters for this data collection also are presented in Table III. No significant variation in intensities of three standards monitored every 50 reflections occurred. A total of 3153 reflections were collected, but only 1682 unique reflections with $I \ge 3\sigma(I)$ were used for structure solution and refinement. These data were corrected for absorption, Lorentz, and polarization effects. Correction for absorption was based on *ϕ* scans of a few suitable reflections with *χ* values near 90° (T_{min}, T_{max} = 0.657, 0.980; μ = 39.0 cm⁻¹). On the basis of systematic absences (hkl, $h + k = 2n + 1$; $h0l$, $l = 2n + 1$) and successful structure solution and refinement, the space group *Cc* was deduced. The structure was solved using the Patterson-superposition technique and refined by a full-matrix least-squares method based on *F* values. Only the W atom was anisotropically described; the other non-hydrogen atoms were refined isotropically. All hydrogen atoms included in the refinement were calculated with C–H = 0.96 Å; C–H–C = 109.4° and fixed at a *U* value of 0.08 Å². The final residuals for variables and independent reflections with $I \ge 3\sigma(I)$ were R = 0.0352 and R_w = 0.0349. The final difference Fourier map had no peak greater than 1.05 e Å⁻³. The final positional parameters were determined with final refinements of the structure with Rogers' *η* value.[21] Scattering factors were taken from ref 22. All calculations were performed on a Micro VAX II computer system using SHELXTL-Plus programs (G. M. Sheldrick, 1990).

Acknowledgment. We thank the National Science Council of the Republic of China (Grant No. NSC 81-0228-M-007-72) for support of this research.

Supplementary Material Available: Tables of atomic positional parameters, all bond distances and angles, thermal parameters, and calculated hydrogen positions for **2a** (5 pages). Ordering information is given on any current masthead page.

OM920718Q

(21) Rogers, D. *Acta Crystallogr.* **1981**, *A37*, 734.
(22) *International Tables for X-ray Crystallography*; Kynoch Press: Birmingham, England, 1974.